

Chapter 2

Carboxylate Based Precursor Systems

Theodor Schneller and David Griesche

2.1 Introduction

Besides the alkoxides described in the preceding chapter, metal carboxylates are the second most frequently employed class of educts which is used for the synthesis of precursor solutions. Chemically they are regarded as derivatives of carboxylic acids which are organic Brönstedt acids of the general formula $R-C(=O)OH$, usually written $R-COOH$ or $R-CO_2H$ where R is a general organic moiety. The length and chemical nature (single or double bonds, linear or branched shape, number and type of hetero atoms etc.) of this organic residue determines the polarity and the decomposition behavior of the acid and the corresponding carboxylate, respectively. Short chain carboxylic acids (1–4 carbons) are soluble in water, whereas longer carboxylic acids are less soluble in polar solvents due to the increasing hydrophobic nature of the longer alkyl chain. These longer chain acids tend to be rather soluble in less-polar solvents such as ethers, alcohols, toluene, xylene etc. Examples for commonly known, simple carboxylic acids are the formic acid $H-COOH$ ($R = H$), that occurs in ants, acetic acid $H_3C-COOH$ ($R = CH_3$), that gives vinegar its sour taste, and butyric acid ($R = CH_3-CH_2-CH_2$) that gives the odor of rancid butter. Acids with two or more carboxyl groups are called dicarboxylic, tricarboxylic, etc. Citric acid is an important example for a tricarboxylic acid and is used in the water based precursor systems described in Chap. 5. The release of the proton (Fig. 2.1) from the carboxylic acid corresponds to the formation of the carboxylate anion, which is stabilized by the negative charge shared (delocalized) between the two oxygen atoms (mesomerism). This means that each of the carbon-oxygen bonds in a carboxylate anion has a partial double-bond character, which is also reflected in the carbon-oxygen bond lengths (~ 136 pm). This value is between

T. Schneller (✉) • D. Griesche

Institut für Werkstoffe der Elektrotechnik II, RWTH Aachen University, Aachen, Germany
e-mail: schneller@iwe.rwth-aachen.de

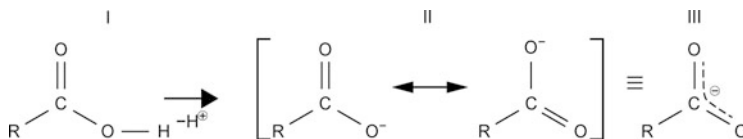


Fig. 2.1 Schematic of the acidity effect of the carboxylic acid (I) which leads to the carboxylate anion (III). This anion is stabilized by mesomerism (II), which is beside the polarity of the O-H bond a further reason for the acidity of carboxylic acids. The free electron pairs may form bondings to metal cations in different modes (see below)

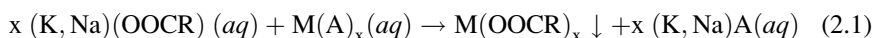
the bond length of a carbon-oxygen double-bond (~ 123 pm) and single-bond (~ 143 pm) [1].

By substituting the acid proton with a metal cation (M^{z+}), metal carboxylates are formed (Fig. 2.2). Thus according to their chemical structure, the carboxyl group can act as a bidentate ligand (Fig. 2.2a) either in a chelating or a bridging mode as shown in Fig. 2.2b [2, 3] and the binding mode can be determined via Fourier transform infrared (FT-IR) spectroscopy [4] (see Chap. 9) for example.

The main reason for the popularity of metal carboxylate precursors is that they are often commercially available, cheap, and insensitive to humidity. Moreover the parent carboxylic acids can be used as solvent and are often less toxic compared to other organic solvents such as 2-methoxyethanol. Although carboxylic acids are weak acids, which means that their negative logarithmic acidity constant pK_a is in the range of 4–6, there is a correlation between the chain length (number of carbon atoms) of the acids and the logarithmic acidity constants [5, 6]. It can be seen in Table 2.1 that the acid strength decreases with increasing chain length. For a more detailed discussion of the properties of metal carboxylates see also [7].

2.1.1 Synthesis Aspects

Several methods have been used to synthesize metal carboxylates [8–11]. One possible synthesis method is the aqueous metathesis. To provide the desired carboxylate ligands, an aqueous solution (*aq*) of the corresponding sodium or potassium carboxylate is prepared. Then another solution containing a salt of the desired metal is added. The metathesis reaction can be described by the following general reaction equation.



Here M represents the particular metal ion and A is the anionic leaving group of the metal salt $M(A)_x$. The metal carboxylate $M(OOCR)_x$ has low solubility in water, especially when its organic moiety R consist of more than six carbon atoms. Hence it can be removed by filtering, washed with an alcohol for example, and dried. Several salts $M(A)_x$ have been used, e.g. copper and lead dodecanoate

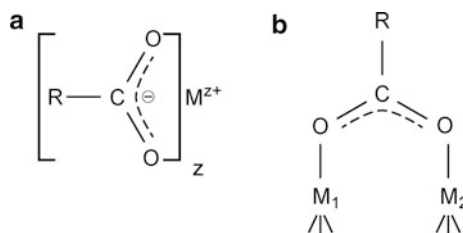


Fig. 2.2 Scheme of different bonding modes of metal carboxylates. In the chelating mode (a) the metal ion is centered between the two oxygen atoms of the carboxylate group and is attracted to both oxygen atoms, whereas in the bridging mode (b) each carboxylate-oxygen atom coordinates to one metal ion, which can be different (M_1 and M_2)

Table 2.1 Negative logarithmic acidity constants (pK_a) for different aliphatic carboxylic acids

| Name of the acid | Number of carbon atoms | pK_a |
|------------------|------------------------|--------|
| Acetic | 2 | 4.76 |
| Propionic | 3 | 4.87 |
| Butyric | 4 | 4.82 |
| Isobutyric | 4 | 4.86 |
| Valeric | 5 | 4.86 |
| Hexanoic | 6 | 4.88 |
| Heptanoic | 7 | 4.89 |
| Octanoic | 8 | 4.89 |
| Nonanoic | 9 | 4.96 |

In the mid column the number of carbon atoms is shown. Taken from [5, 6]

and octadecanoate prepared from the corresponding acetates [9]. Also the sulphates of zinc, magnesium, lead nitrate and calcium chloride were successfully transformed to the octadecenoates by metathesis reactions [10]. A second synthesis route is to treat the metal hydroxides with an alcoholic solution of the carboxylic acid [8]. This method had been used for the preparation of copper, silver, barium, mercury, lead iron cobalt, nickel and alkaline carboxylates [11]. The reaction formula can be given as follows.



The water which is formed in this reaction can be removed by distillation under reduced pressure or by washing with anhydrous solvents. However, this method has several disadvantages, e. g. the resulting carboxylates can be extremely viscous, and hence the filtration is sometimes difficult and non-reacted carboxylic acid can hardly be removed. In case of the carboxylates of lead, mercury, iron and the alkaline earths, a modification of this method leads to better results. The corresponding metal oxide was dissolved in the molten carboxylic acid and the product afterwards is cleaned with hot ethanol and petroleum ether [11]. One requirement of every synthesis is the accurate control of the product stoichiometry and this is related to a well-defined amount of water of constitution. The control of

this issue is not only quite important because the composition of the product directly relies on the used educts. The water of constitution can also change the solution behavior drastically. This is often strongly dependent on the chemical route which is used to prepare the desired metal carboxylate. The following example can serve as an illustration. The metathesis reaction of magnesium chloride with sodium octadecenoate in water yields a precipitate which could be identified as $\text{Mg}(\text{OOC}_{18}\text{H}_{33})_2 \cdot 2 \text{H}_2\text{O}$ [12]. It was only moderately soluble in benzene, but when it was refluxed in dry benzene and then recrystallized, the recrystallization product was found to be $\text{Mg}(\text{OOC}_{18}\text{H}_{33})_2$ and this had better solubility in benzene than the original precipitate [13].

In the following sections details on the use of metal carboxylates as an important class of chemical educts for the synthesis of CSD precursor solutions are described. Emphasis will be given to the carboxylates of alkaline and rare earth elements as well as selected metals from the groups 4 to 14 of the periodic table of elements, since they are relevant for the synthesis of precursor solutions for CSD of ferroelectric, dielectric and conducting perovskite thin films. The coating process for producing thin oxide films from pure carboxylate based precursor solutions is known as metallo-organic-decomposition (MOD),¹ which is an indication that the organic matrix which surrounds the metal ions in the as-deposited films has typically to be removed by thermal decomposition rather than simple in an evaporation process which takes place in case of classical sol-gel processes. The “o” in metallo-organic indicates that the bond formation of the organic ligands occurs via an oxygen atom and not via direct carbon-metal bond as in real metal organic compounds.

On top of syntheses based on only metal carboxylates, solution synthesis routes based on suitable mixtures of metal alkoxides (Chap. 1) and metal carboxylates are also frequently used. Such approaches are often called hybrid-routes and will be described in more detail in subsequent Chap. 3.

2.2 General Considerations of MOD-Processes

Metallo-organic-decomposition is well established and a huge number of inorganic thin films have been made by this technique [14, 15]. In many cases processing routes are based on a hybrid of sol-gel chemistry and MOD-chemistry. A strict separation between the pure sol-gel and the pure MOD chemistry is not always possible, but some important characteristics of “pure” MOD processes will be given in this section. Generally these types of CSD-processes can be divided into a few main steps, which are summarized as flow-chart in the general introduction of this book.

¹ In the literature the phrase “metal organic deposition” is also often used. It denotes the same kind of precursor chemistry.

In the first step, the M-carboxylates are dissolved in a suitable solvent such as the parent acid or xylene. The stoichiometry of the educts and therefore the composition of the resulting layer can be directly adjusted by mixing defined amounts of the prepared solutions or, in some cases, by direct weighting out the carboxylates and alkoxides in one pot followed by dissolution in the desired solvent. The properties of the resulting solutions such as viscosity can be influenced by further chemical or physical modification (distillation, etc.). The precursor solution can be deposited on the substrate by various techniques (e.g. spray coating, spin coating or dip coating, (see Chaps. 11–13) in the second step, where the so called wet film is generated. After this, a certain temperature treatment follows, in which the organic material is removed and a crystalline film is formed. The last two steps can be repeated until the desired layer thickness is achieved. Beside the mentioned often cheap and easy-manageable educts, the main advantage of the carboxylate-based-routines is the comparably low temperature which is needed in the crystallization step to form thermodynamically stable phases. This is because the educt molecules are mixed at the molecular level. Thus, the diffusion paths of the metal- and oxygen-ions are short compared to classical powder based syntheses of ceramic bulk materials. In addition the relatively low temperature often helps to prevent the evaporation of volatile decomposition products. A skillful temperature treatment leads to the possibility of precise control of the microstructure, e.g. grain size and orientation (see Chap. 17). The carboxylates used should fulfill a few requirements:

- The educts should be available as highly pure materials and should possess a defined molecular structure.
- If they are not commercially available, they should be easy to synthesize and purify.
- They should be stable in air in order to facilitate handling.
- The metal content should be high to prevent massive reduction in volume (which can lead to micro cracks in the layers) during pyrolysis and crystallization.
- They should show an adequate solubility in the desired solvent and they should be compatible with each other.
- The decomposition should not lead to the formation of volatile metal containing species, melts, carbon contamination, and toxic gases. This often restricts the choice of the carboxylate chain, because heteroatoms such as, nitrogen, sulphur, or in particular fluorine in the chain lead to highly toxic decomposition gases.

Next, a brief survey of the deposition and thermal treatment is given.

2.2.1 Thin-Film-Deposition and Thermal Treatment: Solvent Evaporation Behavior

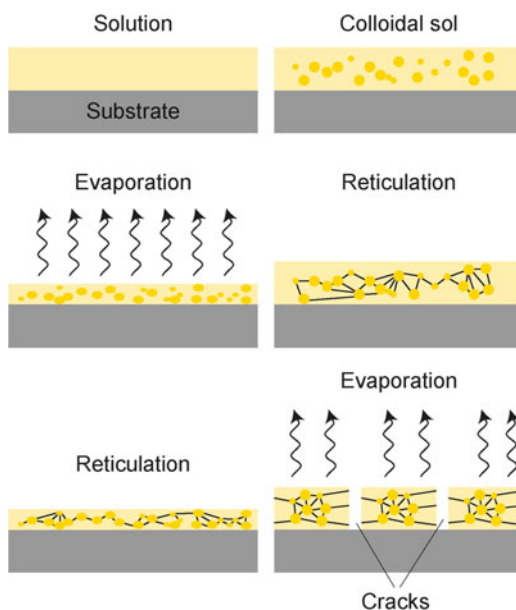
The deposition of a given MOD or hybrid solution is one of the most important steps [14, 15], since it determines the final uniformity of the resulting film to a large

extent, as can be seen in the later chapters (Chaps. 10–12). Spin coating is the most common deposition technique and was adopted from classical semiconductor fabrication technologies, i.e. deposition of photoresists for standard optical lithography. Naturally, the deposition should be carried out in a clean room environment to avoid the contamination of the film by dust particles. Such contaminations might lead to the appearance of dust streaks, which of course degrades the quality of the film. If the deposition process involves any solvent evaporation, the deposition should be very rapid, because the solubilities of the metallo-organic species may be different. Rapid processing might prevent the segregation of the species. In general, there is a direct dependence between the viscosity and the concentration of the metallo-organic species in the solution. With increasing concentration, the viscosity also increases. This effect is relatively strong in MOD-derived solutions in comparison to pure sol-gel processes. Less viscous solutions result in thinner films, i.e. more deposition steps are necessary to achieve thicker films. On the other hand, a lower thickness per coating step may enable the deposition of ultrathin films. A key feature of any deposition method is the ability to control the uniformity and film thickness which is related to the pyrolysis step. Pyrolysis here refers to the removal of the solvent followed by the decomposition of the organic residues through thermal treatment in oxygen containing atmospheres. The spin coating process of a simple MOD-system in a non-volatile Newtonian fluid, where no slip occurs at the liquid-solid interface, can be theoretically expressed using a modified Navier-Stokes equation [16]. Equation (2.3) describes the relation of the film thickness after pyrolysis (h_s) and the physical parameters of the precursor solution:

$$h_s = \frac{c}{2\omega\rho_s} \left(\frac{3\eta\rho_l}{t} \right)^{1/2} \quad (2.3)$$

Here ρ_s and ρ_l are the solid and liquid densities, ω respectively is the angular velocity, t refers to the spinning time, c is the mass concentration of the solution formulation (weight of solid film/weight of solution) and η is the viscosity of the liquid. This equation was verified experimentally with an MOD-derived lead titanate (PTO)-film with lead neodecanoate and titanium di-methoxy-di-neodecanoate as educts and xylene as solvent [15]. The agreement of the theoretically predicted film thickness and the experimentally derived values was notably good. When comparing the pyrolysis of sol-gel routines with MOD-derived films, there are also some significant differences. As described earlier, a MOD-solution can be considered as a system where the metal cations are solvated and complexed by the carboxylate functions. For this reason usually no or very little reticulation occurs between the molecules. Hence it can be said that the hydrocarbon chain of the carboxylate provides a kind of protection due to its hydrophobic nature. By contrast in pure sol-gel routines the precursor-solutions consist of more or less colloidal sols, and depend on the additives for chemical protection. Figure 2.3 shows the different events, which occur when the chemically different precursor solutions are deposited on the surface, and heating starts [17]. The

Fig. 2.3 Schematic comparison of the events which take place when a MOD-derived solution (*left side*) and a colloidal sol (*right side*) are deposited on a certain surface and pyrolysis starts. The main difference is that from a MOD-solution the evaporation starts earlier, followed by the reticulation, whereas in the case of colloidal sols these two events are switched, which may result in the formation of microcracks. Modified after [17]



evaporation of the solvent in MOD-processes occurs perpendicular to the substrate, which leads to a shrinkage in the perpendicular direction. Reticulation occurs later when the decomposition occurs. In the sol-gel process, reticulation starts earlier, e.g. before the evaporation of the solvent [17]. This early onset of reticulation is a consequence of the more reactive nature of the metal alkoxides (the details of which may be found in Chap. 1). Thus shrinkage parallel to the substrate takes place which might result in the formation of microcracks.

Further thermal treatment at higher temperatures results in the decomposition of the organic residues and leads to amorphous or crystalline ceramic thin films, which is explained in the next section.

2.2.2 Decomposition Behavior

If the as-deposited layer is treated at higher temperatures decomposition of organic residues takes place. This step usually results in a large decrease in volume, which may also lead to microcracks. As mentioned before and described in more detail in Chaps. 15 and 17, the thermal treatment determines the evolution of the microstructure and so the heat process has to be optimized for the desired film morphology (dense, porous, fine grained etc.). In particular the heating rates play an important role. In general, a low heating rate during solvent evaporation phase is desirable to prevent cracking. The heating rates in the decomposition and crystallization phase are specific for every given system. Thermogravimetric analysis can

be used to estimate the minimum temperature for decomposition and removal of the organic species. If it is coupled with a differential thermoanalysis, crystallization events are also distinguishable (for details see Chap. 7). The decomposition mechanisms of the carboxylate based precursor solutions are rather complex and not completely understood. A possible mechanism can be deduced from comparisons of thermoanalysis data obtained from decomposition studies of the individual PTO-precursors titanium-dimethoxy-dineodecanoate and lead-ethylhexanoate with a precursor mixture of both components in xylene. It was shown that the decomposition temperature of the individual components was significantly lower than the corresponding temperature for the mixture. This indicates a kind of domino effect in the decomposition process of the mixture. It was assumed that the decomposition of the mixture consists of three steps, in which radical reactions take place. First, free organic radicals are generated through thermal fission. This step is rate determining and followed by a second step that involves fast fragmentation of the organic radicals. The last step is a very fast oxidative chain reaction of the organic radicals to yield longer chains. If this mechanism is valid, the decomposition temperature should decrease with increasing chain length, branching and oxygen partial pressure. Indeed this behavior has been found in most but not all cases [14]. Thus the affirmation of this or other kinds of decomposition mechanism should be the interest of further research. Nevertheless, there are many reports about the decomposition of metal carboxylates as single components [18–34]. Care should be taken when single component decomposition behavior is directly compared with precursor solution decomposition mechanisms, but still the reaction pathways which have been determined for single components are a good starting point for continuative experiments.

In the following sub-sections the behavior of some important examples which concern the commonly used metal carboxylates (acetates, propionates and long-chain carboxylates) are reviewed, followed by selected studies on the decomposition of MOD-mixtures.

2.2.2.1 Metal Acetates and Propionates

Metal acetates can be considered as the most investigated carboxylates with respect to their decomposition behavior [18, 19]. One has to keep in mind the two important considerations in all the analyses of the decomposition processes which can be found in literature. First, metal carboxylates can contain a certain amount of water of constitution. The second point concerns the atmosphere in which the decomposition took place. In some cases the resulting decomposition products differ drastically in their nature according to the atmosphere under which the certain experiment was carried out. In an infrared-spectroscopic study of the decomposition of several metal acetates in air it was found that there are three temperature regions [18]: (a) the temperature of dehydration (80–130 °C), (b) the temperature where intermediates are formed (105–230 °C), and (c) the decomposition temperature (100–440 °C), where the intermediates are converted into the final product.

Based on the above discussion, the metal acetates can be classified by the intermediates and final products that occur. For the alkaline acetates (potassium and sodium), the intermediate is the corresponding oxalate, which decomposes and yields the metal carbonate. For barium acetate the corresponding carbonate occurs directly without an intermediate, whereas calcium acetate decomposes to the carbonate over a crystalline anhydrous modification. Magnesium, lead, nickel, and cadmium acetates form an intermediate basic salt. In case of cadmium, nickel, and lead acetate this intermediate decomposes at higher temperatures to give the metal, while magnesium acetate yields the corresponding metal oxide. The occurrence of the pure metal as final product was also observed for copper acetate, where the decomposition proceeds via a crystalline modification of the anhydrous acetate as the intermediate analogous to the calcium. Cobalt and silver acetate decompose to the pure metal without the formation of an intermediate. Under air all metals are immediately oxidized to form the oxides. The crystalline acetate modification as intermediate is also observed for zinc and manganese acetate, which decompose to the corresponding oxides. It should be noted that the generated carbonates can be transformed into the corresponding oxides at higher temperatures. This happened for example between 350 and 450 °C when anhydrous lead(IV) acetate ($\text{Pb}(\text{OOCCH}_3)_4$) was heat treated in air [20]. The decomposition of a number of rare earth acetates have also been investigated [19–24]. All the investigated rare earth acetates consisted of three acetate ions coordinated to the central metal cation complemented by 1–4 water molecules of constitution per metal ion. This leads to the general formula $\text{Ln}(\text{OOCCH}_3)_3 \cdot x\text{H}_2\text{O}$. Consequently the first reaction was always found to be dehydration at temperatures between 90 and 250 °C. It could elapse in one or more steps. For instance dysprosium acetate $\text{Dy}(\text{OOCCH}_3)_3 \cdot 4\text{H}_2\text{O}$ loses 3.5 molecules of water at 90 °C and the last 0.5 molecule is released at 150 °C [20]. The intermediate is a thermally unstable anhydrous acetate. This anhydrous form can undergo several phase transitions [21], where monodentate, bidentate or even polymeric species can occur. It could be shown that in the temperature range of 250–500 °C the anhydrous acetates were transformed into a broad range of secondary intermediates. These secondary intermediates can be the corresponding oxyacetates, carbonates, oxycarbonates, and even hydroxides [19]. In most cases these intermediates occur in succession. These in turn decomposed then to the oxides in the temperature range from 500 to 900 °C. The structure of the oxide is depending on the nature of the rare earth element. In most cases the sesquioxides (Ln_2O_3) can be found, but for praeosdymium e.g. the dioxide related structure $\text{PrO}_{1.833}$ was found [22].

Relatively less is known about the decomposition behavior of the metal propionates. The decomposition of the monohydrated alkaline earth propionates ($\text{M}(\text{OOCCH}_2\text{CH}_3)_2 \cdot \text{H}_2\text{O}$ with $\text{M} = \text{Ba}, \text{Sr}, \text{and Ca}$) proceeded over a single stage dehydration step for the strontium and calcium propionates and a two stage dehydration step for barium propionate, in which $\text{Ba}(\text{OOCCH}_2\text{CH}_3)_2 \cdot 0.5\text{H}_2\text{O}$ is formed at temperatures lower than 200 °C [25]. The anhydrous propionates crystallize at about 200 °C. Above 300 °C, the decomposition took place simultaneously with melting, resulting in the formation of carbonates at 350 °C.

In another study [26], the decomposition of the self-prepared propionates of nickel ($\text{Ni}(\text{OOCCH}_2\text{CH}_3)_2 \cdot \text{H}_2\text{O}$), cobalt ($\text{Co}(\text{OOCCH}_2\text{CH}_3)_2 \cdot 3\text{H}_2\text{O}$), copper ($\text{Cu}(\text{OOCCH}_2\text{CH}_3)_2 \cdot 0.5\text{H}_2\text{O}$) and zinc ($\text{Zn}(\text{OOCCH}_2\text{CH}_3)_2 \cdot \text{H}_2\text{O}$) was analyzed. It was found that the stepwise dehydration processes took place in the temperature range between 70 and 130 °C to form the anhydrous propionate, and the final decomposition give rise to a few unidentified intermediates in the range of 250–360 °C. In all cases the final products were the corresponding metal oxides. The decomposition behavior of iron propionate trihydrate ($\text{Fe}(\text{OOCCH}_2\text{CH}_3)_3 \cdot 3\text{H}_2\text{O}$) was also investigated [27]. Here it could be shown, that the decomposition of this carboxylate proceeds via the dehydration at 170 °C in one step, followed by the reduction of the Fe(III)-ions to form anhydrous iron(II) propionate at 230 °C. At 570 °C the resulting $\alpha\text{-Fe}_2\text{O}_3$ occurred. For in-situ-prepared nickel propionate and lanthanum propionate interesting differences in the thermospectroscopically detected decomposition behavior could be determined if one was varying the atmospheres in which the heat treatments were carried out [28]. For the nickel propionate it could be shown that by heating in air up to 150 °C, the dehydration process took place, which was followed by the endothermic transformation of the propionate ligands into acetate groups and the decomposition of these between 250 and 325 °C. The exothermic formation of nickel oxide was completed at 325 °C. In contrast, the decomposition to nickel oxide in nitrogen seems to be a complete endothermic process although the temperatures of the different decomposition were found to be only a few degrees lower than in air. In hydrogen atmosphere, a sharp exothermic signal was found due to the reduction of nickel oxide to elemental nickel around 325 °C. Contrary to these results the lanthanum propionate decomposes in air around 325 °C to give a mixture of the corresponding oxide and oxycarbonate. This mixture is transformed into the pure oxide at 720 °C. In nitrogen, only the oxycarbonate was found as intermediate in the temperature region between 250 and 575 °C. The characteristics in hydrogen atmosphere are in this case quite similar to that in nitrogen.

The combustion of rare earth precursors (Ln -propionates $\text{Ln}(\text{OOCCH}_2\text{CH}_3)_3 \cdot x\text{H}_2\text{O}$ with $\text{Ln} = \text{Ho}, \text{Er}, \text{Tm}, \text{and Yb}$) in an argon atmosphere revealed a similar decomposition behavior as discussed above [29]. Dehydration took place around 90 °C and the resulting anhydrous propionates decomposed to give the oxycarbonates ($\text{Ln}_2\text{O}_2\text{CO}_3$) between 300 and 400 °C. In the temperature region of 500–700 °C a mixture of the oxycarbonate and the corresponding sesquioxide (Ln_2O_3) could be detected. The transformation into the sesquioxide was found to be complete around 1,100 °C.

2.2.2.2 Long Chain Metal Carboxylates

The most remarkable difference between long-chain and short chain carboxylates is the onset state of thermal decomposition. While short chain carboxylates tend to decompose from the solid state, the long-chain analogs decompose from the melt [30]. The phase formation behavior and other characteristics of the melts are

discussed elsewhere [30]. The difference due to chain length can be clearly seen in a study involving eight saturated, non-branching sodium carboxylates [31]. The authors found that in air the decomposition temperature decreases from 330 °C for the formate to 190 °C for the tetradecanoate. A similar behavior was found for heating the same carboxylates in nitrogen. However here the decomposition temperatures were slightly higher, which leads to the suggestion of an additional stabilization effect in inert gas atmosphere.

In case of the long-chain lead carboxylates (dodecanoate, tetradecanoate and octadecanoate) it revealed that the decomposition for the do- and tetradecanoate occurred in one step, whereas a two-step mechanism was found for the octadecanoate in all cases between 230 and 460 °C, resulting in lead oxide [32]. Furthermore, the thermal behavior of chromium, copper, nickel, and zinc dodecanoates was investigated [33]. The chromium dodecanoate decomposes via an oxydodecanoate intermediate, whereas the copper dodecanoate forms a temporary mixture of copper oxide and copper dodecanoate. The nickel containing molecule seemed to decompose to the oxide without any intermediate and in the case of zinc the zinc carbonate is transitionally formed. The temperature range for the occurrence of intermediates was found to be from room temperature up to 460 °C, depending on the corresponding metal dodecanoate.

The researchers also investigated the interaction of the described soaps when mixing them with different solvents such as the corresponding alcohol, ester, and amine. In case of the copper and chromium dodecanoate the DTA curves changed when the soaps were mixed with dodecanol. It was concluded that a form of complexation due to hydrogen bonding or electron lone pairs occurred. No comparable interaction was found for the other soaps. In a following study [34] the metal dodecanoate-solvent interaction was further investigated for the chromium, copper, nickel and zinc dodecanoates in combination with dodecanoic acid and octadecanoic acid. It was found that only the chromium salt formed a complex with the stoichiometry of soap/acid close to 2:1. The other soaps did not form such a complex. When heating the dodecanoic salts with octadecanoic acid a metathesis took place. Hence by heating the dodecanoic ligands were replaced by octadecanoic ligands. This behavior was confirmed for all of these metal salts.

In the next sections a general view over established MOD processes is given, with special emphasize on the precursor solution chemistry, the thermal treatment and the resulting thin films.

2.3 Long Chain Versus Short Chain Carboxylates: Solution Behavior and Established Processes

In general long chain carboxylates are popular for MOD type CSD routes since they are moisture insensitive and can be dissolved in relatively chemically inert solvents like toluene or xylene. In these solvents, often also alkoxides may be co-dissolved

which enables the relatively simple preparation of the hybrid solutions. Even if the long chain carboxylates are dissolved in alcohols like butanol, problems relating to hydrolysis are not expected, since the esterification reactions which release water are rather slow due to the lower acid constant of the long chain carboxylic acids (Table 2.1).

Due to the above mentioned advantage, relatively long chain lead(II) 2-ethylhexanoate was used in one of the first synthesis routes to lead zirconate titanate thin films in 1984 [35]. Using this route stable and moisture insensitive precursor solutions have been obtained and this principle has often been used in particular in the early days of PZT [36–38]. It was somewhat later transferred to other materials like yttrium barium copper oxide (YBCO) [39, 40], barium strontium titanate [41, 42], strontium bismuth tantalate [43] etc.

However sometimes problems may occur due to the relatively high content of carbon. This carbon is typically removed by combustion in air resulting in larger portions of carbon dioxide which in turn often leads to some porosity in the films and possibly also to residual carbon. The latter may be detrimental for the leakage properties of these MOD derived ferroelectric thin films [36, 38] or the current transport in superconducting YBCO films [39, 40]. In order to reduce the problematic parasitic carbon incorporation and crack formation short chain carboxylates like acetates or propionates were introduced. A pioneer work with such educts was carried out in 1984 by Heartling [44]. He used dip-coating to synthesize high quality, crack-free PLZT-films, with an average grain size of $\sim 1\text{ }\mu\text{m}$ in diameter. The educts lead, lanthanum, and zirconium as acetate and titanium-acetylacetonate were dissolved in a mixture of water and methanol. The use of water as solvent is often problematic if the used substrates have hydrophobic surfaces and therefore result in poor wetting. To overcome this issue, coating routines with short chain carboxylates were developed which use organic solvents instead of water. Later specific water based precursor systems (Chap. 5) and surface treatments were developed which also led to good coating results.

One good example of the use of short-chained carboxylates is the so called all-propionate-routine (APP), which was first published in 1997 [45, 46]. The authors prepared magnetoresistive alkaline earth metal doped lanthanum manganate thin films with perovskite structure on different substrates. Their precursor solution was made by dissolving the corresponding metal acetates in a mixture of propionic acid and propionic acid anhydride. The propionic acid anhydride was used in this case to remove the water of constitution from the educts. Because the acetate anion is the stronger base than the propionate anion, acetic acid was formed which could be easily distilled off, resulting in the in-situ formation of metal propionates. The authors point out that this routine fulfills the requirements listed in Sect. 2.2. In contrast to other commercially available educts, such as lanthanum acetate, the propionate showed significantly higher solubility. The precursor solution is moisture insensitive, can be easily prepared, and its substrate wetting behavior was found to be excellent. In addition, the stoichiometry of the resulting layer can be varied over a wide range. The decomposition was monitored by infrared spectroscopic analysis. It was found that $\text{La}_2\text{O}_2\text{CO}_3$ and CaCO_3 were the

intermediates formed by the thermal treatment. Dependent on the dopant concentration the crystallization occurred between 650 and 700 °C. The Curie temperature was determined to be -8.1 °C, with a resistivity of $1.6 \Omega\cdot\text{cm}$. This value was higher than for single-crystalline films grown by vapor phase techniques ($\sim 10^{-2} \Omega\cdot\text{cm}$) [47, 48]. The all-propionate route could be used for various other systems, such as LNO [49].

The issues of porosity, residual carbon, and poor leakage current properties are maybe also the reason why only a very few of researchers made use of the the MOD concept to prepare PZT. Most researchers use lead(II) acetate, which was introduced in the first pioneering work of Budd et al. [50] or the oxidized counterpart lead(IV) acetate [51] as the educt for the synthesis of PZT precursor solutions. Although their decomposition temperature is significantly higher than those of the long chain carboxylates (see Sect. 2.2.2.2), they have the benefit of having considerably lower amount of carbon. Another distinct advantage of this synthesis strategy is that Pb-O-M linkages are formed by release of an ester, reducing the amount of carbon in these kind of hybrid solutions (see Chap. 3).

Table 2.2 gives an overview on the most popular carboxylates used for various material systems and corresponding references. Certainly this list is not exhaustive and the reader may find in the literature further examples of less common carboxylates which might be useful for specific precursors.

Shaikh and Vest [70] characterized the PTO and the BTO system made through MOD-routines in a kinetic study. They used titanium(IV)-dimethoxydineodecanoate, barium(II)-neodecanoate, lead(II)-neodecanoate and commercially available lead(II)-acetate for the synthesis. For the BTO-system the barium- and titanium precursors were dissolved and mixed in xylene. XRD and DTA results revealed that the BTO-formation process occurs first by the formation of intermediate large BaCO_3 particles, small TiO_2 -particles and a certain amount of BTO up to a temperature of 600 °C. When the temperature was raised to 660 °C, only BTO was visible in the XRD. Comparing the MOD-route with classic powder syntheses of BTO, the reaction was shown to proceed 500 times faster in the MOD-route at constant temperatures. On the other hand, 900 °C were needed for completing the reaction in powder based synthesis at constant sintering time, while in MOD-syntheses, 660 °C were sufficient. It was concluded that this massive advantage was due to the smaller particle size and the greater homogeneity on the molecular level, as discussed in section 2.2 of this chapter. Because TiO_2 can typically occur in two modifications² (anatase and rutile), two different reaction pathways were possible. The reaction of the rutile phase with BaCO_3 is slower than the reaction of BaCO_3 with the anatase phase. In addition the BaCO_3 -rutile reaction proceeds via Ba_2TiO_4 as intermediate. This intermediate could not be found, which means that the BaCO_3 -anatase pathway was the more probable one.

² It has to be noted, that there is also brookite as third modification possible, which however occurs less frequently in CSD processes.

Table 2.2 Compilation of frequently used carboxyl groups and metal carboxylates, respectively as well as resulting thin film material

| Carboxylate | Metal-cations | Resulting material | References |
|------------------|-------------------------------------|--|--------------|
| Acetate | Pb^{2+} , Pb^{4+} | PTO | [50, 51] |
| | | PZT | |
| | Ca^{2+} , Sr^{2+} | LCMO, LSCO | |
| | Ba^{2+} | BST | [41, 42] |
| | Mn^{2+} | | |
| | Co^{2+} | | |
| | In^{3+} | ITO | [52] |
| Trifluoroacetate | Bi^{3+} | $\text{SrBi}_2\text{Ta}_2\text{O}_9$ | [43] |
| | | $\text{SrBi}_4\text{Ti}_4\text{O}_{15}$ | [53] |
| | Y^{3+} , Cu^{2+} | YBCO | [39, 40] |
| | Ba^{2+} | BTO | [54] |
| Propionate | Pb^{2+} | PZT | [55] |
| | Ba^{2+} , Sr^{2+} | $(\text{Ba}_x, \text{Sr}_{1-x})(\text{Ti}_y, \text{Zr}_{1-y})\text{O}_3$ | [41, 42, 56] |
| | La^{3+} , Ni^{2+} | LNO | [49] |
| | Ca^{2+} | LSCM | |
| | Co^{2+} | LSCO | [57] |
| 2-Ethylhexanoate | Pb^{2+} | | [35, 36] |
| | La^{3+} | | [58] |
| | Zr^{4+} | PLZT | |
| | Ba^{2+} , Sr^{2+} | BaTiO_3 , SrTiO_3 | [59, 60] |
| | Bi^{3+} | Bi(s) | [61] |
| | | $\text{SrBi}_2\text{Ta}_2\text{O}_9$ | [62–65] |
| | | $\text{SrBi}_3\text{Nb}_2\text{O}_9$ | |
| | | $\text{SrBi}_4\text{Ti}_4\text{O}_{15}$ | |
| | In^{3+} , Sn^{2+} | ITO | [66] |
| | Ce^{3+} | CeO_2 | [67] |
| | Y^{3+} | Y_2O_3 | [68] |
| | Fe^{3+} | Fe_2O_3 | [69] |
| Neodecanoate | Pb^{2+} | PTO | [70, 71] |
| | Ba^{2+} | BTO | [72] |
| | Y^{3+} , Cu^{2+} | $\text{YBa}_2\text{Cu}_3\text{O}_{7-x}$ | [39, 40] |

In the PTO-system two Pb-educts were compared. Lead neodecanoate showed a slightly higher volatility than lead acetate. The addition of additives with a high boiling point such as ethyl- or methylstearate to the xylene based precursor solution could solve this problem. At firing temperatures below 625 °C, the two common PbO-modifications (litharge and massicot) and PTO were observed, whereas at temperatures over 625 °C only the PTO-phase was left. The decomposition of lead neodecanoate lead to spherical particles with a uniform size (diameter ~0.3 µm) developed. The decomposition of lead(II) acetate led to irregular shaped particles with diameters between 0.3 and 10 µm. In both cases, there is a TiO_2 -shell on these particles. The larger diameter in the acetate-based system led to a slower long-term kinetics in the formation of BTO, because these larger particles dominate the process at longer firing times.

2.3.1 Another Well-Known Example: Trifluoroacetates

The first working precursor system for the preparation of superconducting YBCO thin films by MOD was found by Kumagai et al. [73]. They mixed yttrium stearate with barium- and copper naphthenate in an organic solvent. The DTA-TG analysis of the resulting precursor solution showed that pyrolytic decomposition took place between 200 and 500 °C followed by crystallization up to 800 °C. Hence the dip coated YSZ substrates were dried in air and fired at 800 °C. They found the quality of the films is directly related to the firing time. This could be evaluated by measuring the transition temperature, T_C (resistance (R) = 0 Ω), e.g. samples fired for 2 h have T_C that were significantly lower (23 K) than samples fired for 80 h (60 K). Although some improvements of the T_C (R = 0 Ω) values could be achieved by the use of other carboxylates and heat treatment procedures [74, 75], the overall electrical properties remained poor owing to the formation of BaCO_3 , which is very stable, as an intermediate compound during the decomposition of the precursors [76], or the inadequate reactivity of the intermediate barium oxide [77].

Thus driven by the necessity to avoid intermediates such as carbonates, metal trifluoroacetates have been introduced in the CSD technology in particular for the preparation of superconducting thin films (see Chap. 27). Gupta et al. [77] therefore dissolved yttrium oxide, barium carbonate and solid copper in aqueous trifluoroacetic acid (TFA) and hydrogen peroxide. These solutions were dried and re-dissolved in methanol. The products of the pyrolysis of the single educts were found to be barium- and yttrium fluoride as well as a mixture of copper oxide and copper fluoride. The mixed educt solutions were spun on YSZ substrates and the annealing was done for 5–40 min in a humid or non-humid helium atmosphere at 850 or 920 °C. The resulting SEM images of the layers revealed large pellet-like, (111)-oriented grains of the superconducting phase with smaller, spheroidal grains lying on them when the samples were sintered without humidification. These small grains were found to be rich in barium. The authors concluded that these grains are barium fluoride, which was corroborated by XRD-measurements. Samples sintered in humid conditions did not show such barium-rich phases and the strict (111)-texture could not be found. Surprisingly, the specimen with barium fluoride-rich grains showed higher transition temperatures (92–94 K) and smaller transient regions. The group proposed that barium fluoride helps the superconducting phase to grow oriented and that maybe there is an additional fluoride substitution. After this study, further investigations of YBCO-layer syntheses were carried out. McIntyre et al. [78] used the described solution process to prepare epitaxial films on (001)-oriented LAO-substrates. They introduced a special kind of temperature treatment which consisted of three parts: a pyrolysis step up to 400 °C, followed by the crystallization at 700 °C, and the oxidation during the re-cooling. Pyrolysis and crystallization were carried out in a humid atmosphere. After the pyrolysis step, the layer consisted of the oxy-fluorides transformed into the tetragonal YBCO-phase during the crystallization. The oxidation led to the orthorhombic superconducting phase. There was a direct relationship between the partial pressure of the oxygen,

the texture development and the transition temperature during the oxidation step; as long as there were used low partial pressures, the XRD showed sharp (001)-reflexes. The transition temperature increases in these samples as well as the transient regions decreased. The described three-step temperature treatment with humid and non-humid atmospheres was more or less adopted by other authors [79–83] and is also relevant for industrial applications (Chap. 27). Yan et al. [81] found another modification of the trifluoroacetate routine by dissolving yttrium, barium, and copper-hydroxides in a mixture of water and TFA. After gelation, they were coated on different substrates and crystallization took place in humid argon at 752 °C. They found an adequate (001)-texture, but the layers were porous with a grain diameter of 1 µm. The transition of these layers was found to be at 91 K with a very small transient region. Obradors et al. systematically investigated the formation of the YBCO thin films on different substrates from TFA-based solutions with the metal acetates as educts [82]. The pyrolysis (up to 300 °C in humid oxygen) was pointed out to be an important step in morphology development. Slow heating rates were found to prevent morphological inhomogeneities. The humid oxygen helps to avoid the sublimation of the $\text{Cu}(\text{TFA})_2$. The crystallization at 700–800 °C in humid oxygen seemed to be a very complex process which needs further investigations. It was supposed that the crystallisation occurs through the formation of a liquid phase at the layer-substrate interface, where the nucleation process in c-direction took place. Also an exchange with the gas phase is important, because the water molecules of the humid atmosphere have to reach the interface. The water reacts there with the in situ formed hydrogen fluoride and removes it. Otherwise hydrogen fluoride would cause a kind of barrier for the further reaction. When temperatures during this process step are too low or the growth rate is too high caused by too high oxygen partial pressure, the crystal growth becomes faster in the a and b-direction, which would lead to porosity formation in the film. The oxidation was performed in dry oxygen at 450 °C. Finally the group could achieve high-quality films without pores and with strict c-orientation. No other phases could have been detected.

Another route was developed by Roma et al. [83]. Instead of TFA, they used the corresponding trifluoroacetic anhydride. In this so called anhydrous TFA route, the YBCO bulk material was directly dissolved in the anhydride, after drying and redissolving in anhydrous methanol a stable solution with a very small content of water was formed. The low water content had the advantage of shortening the pyrolysis step drastically. The slow pyrolysis in the other routes was due to the inhomogeneous distribution of the educt molecules in the solution, which often results in inhomogeneous layers. Water acts as a ligand especially for yttrium trifluoroacetate. This coordination may lead to the mentioned inhomogeneity. Nevertheless, high quality layers could be also made by this routine.

2.4 Summary

In this chapter, the basics of metal carboxylates which is a frequently used class of chemical educts for solution synthesis was first reported. Metal carboxylates offer several advantages in comparison to metal alkoxides, since they are insensitive against moisture and can be produced in a cheap and simple way, e.g. by metathesis reactions. In the second part, the concept of metallo-organic decomposition was introduced, which typically relies on these metal salts and represents a powerful technique for producing ceramic thin films. Concerning the deposition of a given precursor solution and its effect on the film thickness, proportionality to the solution concentration and to the root of the viscosity was found. Problems of substrate wetting can be overcome through the wide range of potential solvents for this routine. The thermal treatment of the as-deposited films leads to solvent evaporation and decomposition of the organic residues. A radical mechanism was proposed to explain the decomposition behavior. Shrinkage of the films parallel to the substrate surface may result in the formation of microcracks. A few examples for the decomposition of selected long-chain and short-chain metal carboxylates illustrated the possibilities. It was shown that the long-chain carboxylates in general decompose at lower temperatures, but the problem of carbon incorporation is reduced when the length of the carbon chain is decreased. Some impressive examples for established MOD processes are given, which resulted in thin films with comparable electrical performances to films which were produced by physical deposition techniques.

In this sense one remarkable research area is the solution based deposition of superconducting YBCO thin films, where fluorinated carboxylates are used to prevent the intermediate formation of carbonates and unreactive oxides. Decomposition and crystallization proceeds via intermediate fluorides and finally yields excellent film qualities. Thus this system is the precursor of choice for commercially CSD produced superconducting layers.

References

1. Clayden J, Greeves N, Warren S, Wothers P (2006) Organic chemistry, 1st edn. Oxford University Press, Oxford
2. Bala T, Prasad BLV, Sastry M, Kahaly MU, Waghmare UV (2007) Interaction of different metal ions with carboxylic acid group: a quantitative study. *J Phys Chem A* 111:6183–6190
3. Boyle TJ, Raymond R, Boye DM, Ottley LAM, Lu P (2011) Structurally characterized luminescent lanthanide zinc carboxylate precursors for Ln–Zn–O nanomaterials. *Dalton Trans* 39:8050–8063
4. Marques EF, Burrows HD, da Graca MM (1998) The structure and thermal behaviour of some long chain cerium(III)carboxylates. *J Chem Soc Faraday Trans* 94:1729–1736
5. Dippy JFJ (1938) Chemical constitution and the dissociation constants of monocarboxylic acids. Part X. Saturated aliphatic acids. *J Chem Soc* 1938:1222–1227

6. Davis MM, Pabo M (1966) Comparative strengths of aliphatic acids and some other carboxylic acids in benzene at 25°C. *J Org Chem* 31:1804–1810
7. Mehrotra RC, Bohra R (1983) *Metal carboxylates*, 1st edn. Academic, London
8. Pilpel N (1963) Properties of organic solutions of heavy metal soaps. *Chem Rev* 63:221–234
9. Piper JD, Fleiger AG, Smith CC, Kerstein NA (1939) Chemical, physical, electrical properties of systems containing lead or copper soaps in liquid paraffin. *Ind Eng Chem* 31:307–311
10. Nelson SM, Pink RC (1954) Solutions of metal soaps in organic solvents. Part IV. Direct-current conductivity in solutions of some metal oleates in toluene. *J Chem Soc* 1954:4412–4417
11. Lawrence ASC (1938) The metal soaps and the gelation of their paraffin solutions. *Trans Faraday Soc* 34:660–677
12. Parke JB (1934) The phase volume theory and the homogenisation of concentrated emulsions. Part II. *J Chem Soc* 1934:1112–1115
13. Pink RC (1938) 237. Studies in water-in-oil emulsions. Part I. Preparation of anhydrous magnesium oleate. *J Chem Soc* 1938:1252–1254
14. Vest RW (1990) Metallo-organic decomposition (MOD) processing of ferroelectric and electro-optic films: a review. *Ferroelectrics* 102:53–68
15. Vest RW, Vest GM (1989) Metallo-organic decomposition process for dielectric films. DTIC Annual Report for the period 4/1/88 – 3/31/89 on contract No. N00014-83-K-0321, pp 1–59
16. Yanagisawa M (1987) Slip effect for thin liquid film on a rotating disk. *J Appl Phys* 61:1034–1037
17. Gaucher P, Faure SP, Barboux P (1992) Ferroelectric thin film research in France. *Integr Ferroelectrics* 1:353–362
18. Baraldi P (1981) Thermal behavior of metal carboxylates: III-metal acetates. *Spectrochim Acta, Part A* 38:51–55
19. Hussein GAM (1996) Rare earth metal oxides: formation, characterization and catalytic activity. Thermoanalytical and applied pyrolysis review. *J Anal Appl Pyrolysis* 37:111–149
20. Hussein GAM, Kroenke WJ, Goda B, Miyaji K (1997) Formation of dysprosium oxide from the thermal decomposition of hydrated dysprosium acetate and oxalate. Thermoanalytical and microscopic studies. *J Anal Appl Pyrolysis* 39:35–51
21. Adachi G, Secco EA (1972) Thermal transformation in anhydrous rare earth acetates. *Can J Chem* 50:3100–3103
22. Hussein GAM (1994) Formation of praseodymium oxide from the thermal decomposition of hydrated praseodymium acetate and oxalate. *J Anal Appl Pyrolysis* 29:89–102
23. Patil KC, Chandrasekar GV, George MV, Rao CNR (1968) Infrared spectra and thermal decompositions of metal acetates and dicarboxylates. *Can J Chem* 46:257–265
24. Hussein GAM (1994) Spectrothermal investigation of the decomposition course of lanthanum acetate hydrate. *J Therm Anal* 42:1091–1102
25. Gobert-Ranchoux E, Charbonnier F (1977) Comportement thermique des propionates hydrates de calcium, strontium et baryum. *J Thermal Anal* 12:33–42
26. Bassi PS, Jamwal HS, Randhawa BS (1983) Comparative study of the thermal analyses of some transition metal (II) propionates. Part I. *Thermochim Acta* 71:15–24
27. Bassi PS, Randhawa BS, Jamwal HS (1983) Mössbauer study of the thermal decomposition of some iron (III) monocarboxylates. *Thermochim Acta* 62:209–216
28. Kaddouri A, Mazzocchi C (2002) Thermoanalytic study of some metal propionates synthesised by sol–gel route: a kinetic and thermodynamic study. *J Anal Appl Pyrolysis* 65:253–267
29. Grivel JC (2012) Thermal decomposition of $\text{Ln}(\text{C}_2\text{H}_5\text{CO}_2)_3 \cdot \text{H}_2\text{O}$ (Ln = Ho, Er, Tm, and Yb). *J Therm Anal Calorim* 109:81–88
30. Akanni MS, Okoh EK, Burrows HD, Ellis HA (1992) The thermal behavior of divalent and higher valent metal soaps: a review. *Thermochim Acta* 208:1–41
31. Roth J, Meisel T, Seybold K, Halmos Z (1976) Investigation of the thermal behavior of fatty acid sodium salts. *J Thermal Anal* 10:223–232

32. Ellis EA (1981) Kinetics and reaction mechanism for the thermal decomposition of some even chain lead(II) carboxylates. *Thermochim Acta* 47:261–270
33. Seddon AB, Wood JA (1986) Thermal studies of heavy-metal carboxylates. II. Thermal behavior of dodecanoates. *Thermochim Acta* 106:341–354
34. Seddon AB, Wood JA (1987) Thermal studies of heavy-metal carboxylates. III. Metal dodecanoate-carboxylic acid mixtures. *Thermochim Acta* 118:253–260
35. Fukushima J, Kodaira K, Matsushita T (1984) Preparation of ferroelectric PZT films by thermal decomposition of organometallic compounds. *J Mater Sci* 19:595–598
36. Klee M, Eusemann R, Waser R, Brand W, van Hal H (1992) Processing and electrical properties of $\text{Pb}(\text{Zr}_x\text{Ti}_{1-x})\text{O}_3$ ($x=0.2-0.75$) films: comparison of metallo-organic decomposition and sol-gel processes. *J Appl Phys* 72:1566–1576
37. Chen SY, Chen IW (1994) Temperature-time texture transition of $\text{Pb}(\text{Zr}_{1-x}\text{Ti}_x)\text{O}_3$ thin films: I. Role of Pb-rich intermediate phases. *J Am Ceram Soc* 77:2332–2336
38. Chen SY, Chen IW (1997) Comparative role of metal-organic decomposition-derived [100] and [111] in electrical properties of $\text{Pb}(\text{Zr}, \text{Ti})\text{O}_3$ thin films. *Jpn J Appl Phys* 36:4451–4458
39. Mantese JV, Hamdi AH, Micheli AL, Chen YL, Wong CA, Johnson JL, Karmarkar MM, Padmanabhan KR (1988) Rapid thermal annealing of high T_C superconducting thin films formed by metalorganic deposition. *Appl Phys Lett* 52:1631–1633
40. Hamdi AH, Mantese JV, Micheli AL, Laugal RCO, Dungan DF, Zhang ZH, Padmanabhan KR (1987) Formation of thin-film high T_C superconductors by metalorganic deposition. *Appl Phys Lett* 51:2152–2154
41. Hasenkox U, Hoffmann S, Waser R (1998) Influence of precursor chemistry on the formation of MTiO_3 ($M = \text{Ba}, \text{Sr}$) ceramic thin films. *J Sol-Gel Sci Technol* 12:67–79
42. Hoffmann S, Waser R (1999) Control of the morphology of CSD-prepared $(\text{Ba}, \text{Sr})\text{TiO}_3$ thin films. *J Eur Ceram Soc* 19:1339–1343
43. Boyle TL, Buchheit CD, Rodriguez MA, Al-Shareef HN, Hernandez BH, Scott B, Ziller JW (1996) Formation of $\text{SrBi}_2\text{Ta}_2\text{O}_9$: Part I. Synthesis and characterization of a novel “sol-gel” solution for production of ferroelectric $\text{SrBi}_2\text{Ta}_2\text{O}_9$ thin films. *J Mater Res* 11:2274–2281
44. Heartling GE (1991) PLZT thin films prepared from acetate precursors. *Ferroelectrics* 116:51–63
45. Hasenkox U, Mitze C, Waser R (1997) A novel propionate-based chemical solution deposition method of $\text{La}_{1-x}(\text{Ca}, \text{Sr})_x\text{MnO}_3$ thin films for microelectronics applications. *Integr Ferroelectr* 18:339–350
46. Hasenkox U, Mitze C, Waser R (1997) Metal propionate synthesis of magnetoresistive $\text{La}_{1-x}(\text{Ca}, \text{Sr})_x\text{MnO}_3$ thin films. *J Am Ceram Soc* 80:2709–2713
47. Gupta A, McGuire TR, Duncombe PR, Rupp M, Sun JZ, Gallagher WJ, Xiao G (1995) Growth and giant magnetoresistance properties of La-deficient $\text{La}_x\text{MnO}_{3-\delta}$ ($0.67 \leq x \leq 1$) films. *Appl Phys Lett* 67:3494–3496
48. Snyder GJ, Hiskes R, DiCarolis S, Beasley MR, Geballe TH (1996) Intrinsic electrical transport and magnetic properties of $\text{La}_{0.67}\text{Ca}_{0.33}\text{MnO}_3$ and $\text{La}_{0.67}\text{Sr}_{0.33}\text{MnO}_3$ MOCVD thin films and bulk material. *Phys Rev B* 53:14434–14444
49. Reichmann K, Schneller T, Hoffmann-Eifert S, Hasenkox U, Waser R (2001) Morphology and electrical properties of SrTiO_3 -films on conductive oxide films. *J Eur Ceram Soc* 21:1597–1600
50. Budd KD, Dey SK, Payne DA (1985) Sol-gel processing of PbTiO_3 , PbZrO_3 , PZT, and PLZT thin films. *Br Ceram Proc* 36:107–122
51. Schwartz RW, Bunker BC, Dimos DB, Assink RA, Tuttle BA, Tallant DR, Weinstock IA (1992) Solution chemistry effects in $\text{Pb}(\text{Zr}, \text{Ti})\text{O}_3$ thin film processing. *Integr Ferroelectrics* 2:243–254
52. Dippel AC, Schneller T, Gerber P, Waser R (2007) Morphology control of highly-transparent indium tin oxide thin films prepared by a chlorine-reduced metallo-organic decomposition technique. *Thin Solid Films* 515:3797–3801

53. Kambara H, Schneller T, Sakabe Y, Waser R (2009) Dielectric properties of highly c-axis oriented chemical solution deposition derived $\text{SrBi}_4\text{Ti}_4\text{O}_{15}$ thin films. *Phys Stat Sol (a)* 206:157–166
54. Fujihara S, Schneller T, Waser R (2004) Interfacial reactions and microstructure of BaTiO_3 films prepared using fluoride precursor method. *Appl Surf Sci* 221:178–183
55. Schneller T, Waser R (2007) Chemical modifications of $\text{Pb}(\text{Zr}_{0.3}\text{Ti}_{0.7})\text{O}_3$ precursor solutions and their influence on the morphological and electrical properties of the resulting thin films. *J Sol-Gel Sci Technol* 42:337–352
56. Halder S, Schneller T, Böttger U, Waser R (2005) Fabrication and electrical characterisation of Zr-substituted BaTiO_3 thin films. *Appl Phys A* 81:25–29
57. Hasenkox U, Waser R (1999) Microstructure and properties of highly oriented PZT thin films on epitaxial ceramic electrodes prepared by CSD. *Ferroelectrics* 225:107–115
58. Vest RW, Lu J (1989) Preparation and properties of PLZT films from metallo-organic precursors. *Ferroelectrics* 93:21–29
59. Braunstein G, Paz-Pujalt GR, Mason MG, Blanton T, Barnes CL, Margevich D (1993) The processes of formation and epitaxial alignment of SrTiO_3 thin films prepared by metallo-organic decomposition. *J Appl Phys* 73:961–970
60. Ousi-Benomar W, Xue SS, Lessard RA, Singh A, Wu ZL, Kuo PK (1994) Structural and optical characterization of BaTiO_3 thin films prepared by metal-organic deposition from barium 2-ethylhexanoate and titanium dimethoxy dineodecanoate. *J Mater Res* 9:970–979
61. Shen WN, Dunn B, Moore CD, Goorsky MS, Radetic T, Gronsky R (2000) Synthesis of nanoporous bismuth films by liquid-phase deposition. *J Mater Chem* 10:657–662
62. Chung CW, Chung I (1999) Effect of pre-annealing on physical and electrical properties of $\text{SrBi}_2\text{Ta}_2\text{O}_9$ thin films prepared by chemical solution deposition. *Thin Solid Films* 354:111–117
63. Desu SB, Joshi PC, Zhang X, Ryu SO (1997) Thin films of layered-structure $(1-x)\text{SrBi}_2\text{Ta}_2\text{O}_9-x\text{Bi}_3\text{Ti}(\text{Ta}_{1-y}\text{Nb}_y)\text{O}_9$ solid solution for ferroelectric random access memory devices. *Appl Phys Lett* 71:1041–1043
64. Amanuma K, Hase T, Miyasaka Y (1995) Preparation and ferroelectric properties of $\text{SrBi}_2\text{Ta}_2\text{O}_9$ thin films. *Appl Phys Lett* 66:221–223
65. Watanabe H, Mihara T, Yoshimori H, Paz de Araujo CA (1995) Preparation of ferroelectric thin films of bismuth layer structured compounds. *Jpn J Appl Phys* 34:5240–5244
66. Xu JJ, Shaikh AS, Vest RW (1988) Indium tin oxide films from metallo-organic precursors. *Thin Solid Films* 161:273–280
67. Morlens S, Ortega L, Rousseau B, Phok S, Deschanvre JL, Chaudouet P, Odier P (2003) Use of cerium ethylhexanoate solutions for preparation of CeO_2 buffer layers by spin coating. *Mater Sci Eng B* 104:185–191
68. Apblett AW, Long JC, Walker EH, Johnston MD, Schmidt KJ, Yarwood LN (1994) Metal organic precursors for Ytria. Phosphorus, Sulfur Silicon Relat Elem 93–94:481–482
69. Xue S, Ousi-Benomar W, Lessard RA (1994) $\alpha\text{-Fe}_2\text{O}_3$ thin films prepared by metalorganic deposition (MOD) from Fe(III) 2-ethylhexanoate. *Thin Solid Films* 250:194–201
70. Shaikh AS, Vest GM (1986) Kinetics of BaTiO_3 and PbTiO_3 formation from metallo-organic precursors. *J Am Ceram Soc* 69:682–688
71. Vest RW, Xu J (1988) PbTiO_3 films from metalloorganic precursors. *IEEE Trans Ultrason Ferroelec Freq Contr* 35:711–717
72. Xu J, Shaikh AS, Vest RW (1989) High k BaTiO_3 films from metalloorganic precursors. *IEEE Trans Ultrason Ferroelec Freq Contr* 36:307–312
73. Kumagai T, Yokota H, Kawaguchi K (1987) Preparation of superconducting $\text{YBa}_2\text{Cu}_3\text{O}_{7-\delta}$ thin films by the dipping-pyrolysis process using organic acid salts. *Chem Lett* 16:1645–1646
74. Klee M, Brand W, DeVries JWC (1988) Superconducting films in the Y-Ba-Cu-O system made by thermal decomposition of metal carboxylates. *J Cryst Growth* 91:346–351

75. Chen YL, Mantese JV, Hamdi AH, Micheli AL (1989) Microstructure and superconducting properties of Y-Ba-Cu-O and Yb-BaCu-O thin films formed by metalorganic deposition. *J Mater Res* 4:1065–1071
76. Parmigiani E, Chiarello G, Ripamonti N, Goretzki H, Roli U (1987) Observation of carboxylic groups in the lattice of sintered $\text{Ba}_2\text{YCu}_3\text{O}_{7-y}$ high- T_c superconductors. *Phys Rev B* 36:7148–7150
77. Gupta A, Jagannathan R, Cooper EI, Giess EA, Landman JI, Hussey BW (1988) Superconducting oxide films with high transition temperature prepared from metal trifluoroacetate precursors. *Appl Phys Lett* 52:2077–2079
78. McIntyre PC, Cima MJ, Smith JA, Hallock RB, Siegal MP, Phillips JM (1992) Effect of growth conditions on the preparation and morphology of chemically derived epitaxial thin films of $\text{YBa}_2\text{Cu}_3\text{O}_{7-x}$ on (001) LAO. *J Appl Phys* 71:1868–1877
79. Sathyamurthy S, Salama K (1999) Processing of Y123 coated conductors using metal organic decomposition. *IEEE Trans Appl Supercond* 9:1971–1974
80. Sathyamurthy S, Salama K (2000) Application of metal-organic decomposition techniques for the deposition of buffer layers and Y123 for coated-conductor fabrication. *Physica C* 329:58–68
81. Yan G, Liu CF, Feng Y, Zhang PX, Wu XZ, Zhou L (2003) New metal organic deposition method using trifluoroacetate for fabrication on YBCO thick film on metal tape. *Physica C* 913:3292–3296
82. Obrardors X, Puig T, Pomar A, Sandiumenge F, Piñol S, Mestres N, Castano O, Coll M, Cavallaro A, Palau A, Gazquez J, Gonzales JC, Gutierrez J, Roma N, Ricart S, Moreto JM, Rossel MD, van Tendeloo G (2004) Chemical solution deposition: a path towards low cost coated conductors. *Supercond Sci Technol* 17:1055–1064
83. Roma N, Morlens S, Ricart S, Zalamova K, Moreto JM, Pomar A, Puig T, Obrardors X (2006) Acid anhydrides: a simple route to highly pure organometallic solutions for superconducting films. *Supercond Sci Technol* 19:521–527

Chemical Solution Deposition of Functional Oxide Thin
Films

Schneller, T.; Waser, R.; Kosec, M.; Payne, D. (Eds.)

2013, XVII, 796 p. 390 illus., 133 illus. in color.,

Hardcover

ISBN: 978-3-211-99310-1